screening assays have been reported recently. One is yeast based,[27] one uses ScN2a cells,[10] and the other is based on fluorescence correlation spectroscopy.[28] These assays are suitable for high-throughput screening of large compound libraries to identify novel lead molecules. The SPR method reported here, which easily assayed interactions between compounds and PrP molecules within less than 3 min per compound, is applicable to high-throughput *in vitro* assay for screening of large compound libraries if more highly performing SPR machines are used. The usefulness of this method in screening for PrP binding ligands is also reported very recently by other researchers.[29]

Two chemicals, ThT and diazepam, showed high binding response but did not inhibit PrPres formation within a non-toxic dose range. Of them, ThT exhibited very low or no affinity with PrP121—231 but the next highest binding response to QC. This suggests that ThT might interact with PrP121—231 non-specifically. For diazepam, similar non-specific interaction with PrP121—231 might be occurred, or the interaction might be specific but unrelated to conversion to PrPres. These inferences, however, remain unsupported by other experimental results obtained here.

On the other hand, such high-affinity compounds as CR and PcTS showed large amounts of binding to PrP121—231. One possible interpretation for this is that the compounds might have two or more binding sites per molecule. In fact, structure–activity relationship analysis for these symmetrical compounds indicates that either half of the molecule has anti-prion activity (Doh-ura K, unpublished data), and their sensorgrams looked very similar to those of anti-PrP antibodies (data not shown). The other is that the compounds might self-assemble to interact with the PrP molecule. It has long been known that CR and many other bis-azo dyes self-assemble in water solutions, and this property is proposed to associate with binding capability.[30]

Instead of the full length of mouse PrP, a carboxy-terminal domain of mouse PrP (PrP121—231) was used in the study because of instability of the full length PrP during the experiment. This carboxy-terminal domain is the only autonomous folding unit of PrP with a defined three-dimensional structure[19,23,24] and contains epitopes recognized by a majority of antibodies bearing anti-prion activity.[31—37] Taken together with our findings suggesting that most of anti-prion compounds might exert their effects by interacting with this domain, targeting the carboxy-terminal domain should not necessarily be either inefficient or inappropriate for looking for new anti-prion compounds.

In conclusion, our study indicated that most anti-prion compounds tested here interacted with and had an affinity for recombinant PrP121—231. The SPR binding response to the PrP121—231 correlated with the anti-prion activity in ScNB cells. These observations will allow further discovery of new classes of anti-prion compounds using the SPR assay.

Acknowledgements This study was supported by grants to K.D. from the Ministry of Health, Labour and Welfare (H16-kokoro-024) and the Ministry of Education, Culture, Sports, Science and Technology (14021085), Japan. The authors thank Dr. Kenta Teruya for critical review of the manuscript.

REFERENCES

1) Prusiner S. B., *Science*, **252**, 1515—1522 (1991).
2) Will R. G., Ironside J. W., Zeidler M., Cousens S. N., Estibeiro K., Alperovitch A., Poser S., Pocchiari M., Smith P. G., *Lancet*, **347**, 921—925 (1996).
3) Brown P., Preece M., Brandel J. P., Sato T., McShane L., Zerr I., Fletcher A., Will R. G., Pocchiari M., Cashman N. R., d'Aignaux J. H., Cervenakova L., Fradkin J., Schonberger L. B., Collins S. J., *Neurology*, **55**, 1075—1081 (2000).
4) Caughey B., Race R. E., *J. Neurochem.*, **59**, 768—771 (1992).
5) Demaimay R., Chesebro B., Caughey B., *Arch. Virol. Suppl.*, **16**, 277—283 (2000).
6) Rudyk H., Vasiljevic S., Hennion R. M., Birkett C. R., Hope J., Gilbert I. H., *J. Gen. Virol.*, **81**, 1155—1164 (2000).
7) Doh-ura K., Iwaki T., Caughey B., *J. Virol.*, **74**, 4894—4897 (2000).
8) Korth C., May B. C., Cohen F. E., Prusiner S. B., *Proc. Natl. Acad. Sci. U.S.A.*, **98**, 9836—9841 (2001).
9) Ryou C., Legname G., Peretz D., Craig J. C., Baldwin M. A., Prusiner S. B., *Lab. Invest.*, **83**, 837—843 (2003).
10) Kocisko D. A., Baron G. S., Rubenstein R., Chen J., Kuizon S., Caughey B., *J. Virol.*, **77**, 10288—10294 (2003).
11) Murakami-Kubo I., Doh-ura K., Ishikawa K., Kawatake S., Sasaki K., Kira J., Ohta S., Iwaki T., *J. Virol.*, **78**, 1281—1288 (2004).
12) Ishikawa K., Doh-ura K., Kudo Y., Nishida N., Murakami-Kubo I., Ando Y., Sawada T., Iwaki T., *J. Gen. Virol.*, **85**, 1785—1790 (2004).
13) Poli G., Martino P. A., Villa S., Carcassola G., Giannino M. L., Dal-l'Ara P., Pollera C., Iussich S., Tranquillo V. M., Bareggi S., Mantegazza P., Ponti W., *Arzneim-Forsch.*, **54**, 406—415 (2004).
14) Sellarajah S., Lekishvili T., Bowring C., Thompsett A. R., Rudyk H., Birkett C. R., Brown D. R., Gilbert I. H., *J. Med. Chem.*, **47**, 5515—5534 (2004).
15) Caughey B., Brown K., Raymond G. J., Katzenstein G. E., Thresher W., *J. Virol.*, **68**, 2135—2141 (1994).
16) Vogtherr M., Grimme S., Elshorst B., Jacobs D. M., Fiebig K., Griesinger C., Zahn R., *J. Med. Chem.*, **46**, 3563—3564 (2003).
17) Caughey W. S., Raymond L. D., Horiuchi M., Caughey B., *Proc. Natl. Acad. Sci. U.S.A.*, **95**, 12117—12122 (1998).
18) Forloni G., Iussich S., Awan T., Colombo L., Angeretti N., Girola L., Bertani I., Poli G., Caramelli M., Grazia Bruzzone M., Farina L., Limido L., Rossi G., Giaccone G., Ironside J. W., Bugiani O., Salmona M., Tagliavini F., *Proc. Natl. Acad. Sci. U.S.A.*, **99**, 10849—10854 (2002).
19) Hornemann S., Glockshuber R., *J. Mol. Biol.*, **261**, 614—619 (1996).
20) Liemann S., Glockshuber R., *Biochemistry*, **38**, 3258—3267 (1999).
21) Johnsson B., Lofas S., Lindquist G., *Anal. Biochem.*, **198**, 268—277 (1991).
22) Myszka D. G., *J. Mol. Recognit.*, **12**, 279—284 (1999).
23) Hornemann S., Korth C., Oesch B., Riek R., Wider G., Wuthrich K., Glockshuber R., *FEBS Lett.*, **413**, 277—281 (1997).
24) Riek R., Hornemann S., Wider G., Billeter M., Glockshuber R., Wuthrich K., *Nature* (London), **382**, 180—182 (1996).
25) Frostell-Karlsson A., Remaeus A., Roos H., Andersson K., Borg P., Hamalainen M., Karlsson R., *J. Med. Chem.*, **43**, 1986—1992 (2000).
26) Tagliavini F., Forloni G., Colombo L., Rossi G., Girola L., Canciani B., Angeretti N., Giampaolo L., Peressini E., Awan T., De Gioia L., Ragg E., Bugiani O., Salmona M., *J. Mol. Biol.*, **300**, 1309—1322 (2000).
27) Bach S., Talarek N., Andrieu T., Vierfond J. M., Mettey Y., Galons H., Dormont D., Meijer L., Cullin C., Blondel M., *Nat. Biotechnol.*, **21**, 1075—1081 (2003).
28) Bertsch U., Winklhofer K. F., Hirschberger T., Bieschke J., Weber P., Hartl F. U., Tavan P., Tatzelt J., Kretzschmar H. A., Giese A., *J. Virol.*, **79**, 7785—7791 (2005).
29) Touil F., Pratt S., Mutter R., Chen B., *J. Pharm. Biomed. Anal.*, **40**, 822—832 (2006).
30) Skowronek M., Roterman I., Konieczny L., Stopa B., Rybarska J., Piekarska B., *J. Comput. Chem.*, **21**, 656—667 (2000).
31) Horiuchi M., Caughey B., *EMBO J.*, **18**, 3193—3203 (1999).
32) Heppner F. L., Musahl C., Arrighi I., Klein M. A., Rulicke T., Oesch B., Zinkernagel R. M., Kalinke U., Aguzzi A., *Science*, **294**, 178—182 (2001).
33) Enari M., Flechsig E., Weissmann C., *Proc. Natl. Acad. Sci. U.S.A.*, **98**, 9295—9299 (2001).

34) Peretz D., Williamson R. A., Kaneko K., Vergara J., Leclerc E., Schmitt-Ulms G., Mehlhorn I. R., Legname G., Wormald M. R., Rudd P. M., Dwek R. A., Burton D. R., Prusiner S. B., *Nature* (London), **412**, 739—743 (2001).
35) White A. R., Enever P., Tayebi M., Mushens R., Linehan J., Brandner S., Anstee D., Collinge J., Hawke S., *Nature* (London), **422**, 80—83 (2003).
36) Féraudet C., Morel N., Simon S., Volland H., Frobert Y., Créminon C., Vilette D., Lehmann S., Grassi J., *J. Biol. Chem.*, **280**, 11247—11258 (2005).
37) Miyamoto K., Nakamura N., Aosasa M., Nishida N., Yokoyama T., Horiuchi H., Furusawa S., Matsuda H., *Biochem. Biophys. Res. Commun.*, **335**, 197—204 (2005).

Available online at www.sciencedirect.com
SCIENCE DIRECT®
Journal of Clinical Neuroscience 13 (2006) 661–665
Journal of Clinical Neuroscience
www.elsevier.com/locate/jocn

Laboratory study

14-3-3 protein levels and isoform patterns in the cerebrospinal fluid of Creutzfeldt-Jakob disease patients in the progressive and terminal stages

Yusei Shiga [a,*], Hideki Wakabayashi [b], Koichi Miyazawa [a], Hiroshi Kido [b], Yasuto Itoyama [a]

[a] *Department of Neurology, Tohoku University School of Medicine, 1-1 Seiryo-machi, Aoba-ku, 980-8574 Sendai, Japan*
[b] *Division of Enzyme Chemistry, Institute for Enzyme Research, University of Tokushima, Tokushima, Japan*

Received 17 May 2005; accepted 23 September 2005

Available online at www.sciencedirect.com
SCIENCE DIRECT
Journal of Clinical Neuroscience 13 (2006) 661–665
Journal of Clinical Neuroscience
www.elsevier.com/locate/jocn

Laboratory study

14-3-3 protein levels and isoform patterns in the cerebrospinal fluid of Creutzfeldt-Jakob disease patients in the progressive and terminal stages

Yusei Shiga [a,*], Hideki Wakabayashi [b], Koichi Miyazawa [a], Hiroshi Kido [b], Yasuto Itoyama [a]

[a] *Department of Neurology, Tohoku University School of Medicine, 1-1 Seiryo-machi, Aoba-ku, 980-8574 Sendai, Japan*
[b] *Division of Enzyme Chemistry, Institute for Enzyme Research, University of Tokushima, Tokushima, Japan*

Received 17 May 2005; accepted 23 September 2005

Abstract

To elucidate the diagnostic value and to establish the 14-3-3 isoform patterns in the cerebrospinal fluid (CSF) of Creutzfeldt-Jakob disease (CJD) patients, we analysed the 14-3-3 isoform patterns in the CSF of 11 CJD patients using the Western immunoassay technique. 14-3-3 protein was detected in the CSF of seven CJD patients in the progressive stage, but not in four patients in the terminal stages whose brains were severely atrophied. The amount of 14-3-3 protein measured semi-quantitatively in the CSF was correlated with that of neuron-specific enolase measured using an enzyme-linked immunosorbent assay in the same CSF. CJD patients showed five dominant 14-3-3 isoforms, γ, ε, ζ, η and β, but 14-3-3 τ, which mainly originates from T lymphocytes, was not detected. 14-3-3 protein is released into the CSF as a consequence of the extensive and rapid destruction of the brain, and the presence of the five isoforms enhances the diagnostic value of 14-3-3 protein in the progressive stage.

Keywords: Creutzfeldt-Jakob disease; 14-3-3 protein; Isoform pattern; Neuron-specific enolase

1. Introduction

The detection of 14-3-3 protein in cerebrospinal fluid (CSF) is an important premortem immunoassay marker to support the diagnosis of Creutzfeldt-Jakob disease (CJD)[1] and is included in the World Health Organization (WHO) diagnostic criteria.[2] However, positive detection has been reported in various neurological disorders other than CJD,[3] and such misleading results could lead to an erroneous diagnosis.[4]

14-3-3 protein has seven isoforms,[5] and six isoforms have been detected in the mammalian brain.[6] The 14-3-3 isoform patterns in the CSF of CJD patients have been reported,[7,8] but the results are controversial, probably because of the inadequate isoform-specificities of the antibodies used in the experiments. To elucidate the diagnostic value of and to establish the 14-3-3 isoform pattern in the CSF of CJD patients, we evaluated the isoform patterns in the CSF of CJD patients in the progressive and terminal stages by using highly isoform-specific antibodies against 14-3-3 protein.[9]

2. Methods

We collected CSF from 11 CJD patients, including two familial cases of CJD with no family history of CJD nor dementia, and one patient who had received cadaveric dura mater during surgical resection of a right acoustic neurinoma. The patients were aged between 55 and 79 years, with a mean age of 70.4 years. Seven were diagnosed with probable CJD, and four were definite cases based on the WHO diagnostic criteria.[2] In the seven patients with probable CJD (patients 1 to 7), lumbar CSF was collected in the progressive stage 1–6 months after onset, when the patients were admitted to our hospital, and was stored at −80 °C

* Corresponding author. Tel.: +81 22 717 7189; fax: +81 22 717 7192.
E-mail address: yshiga@em.neurol.med.tohoku.ac.jp (Y. Shiga).

0967-5868/$ - see front matter © 2006 Elsevier Ltd. All rights reserved.
doi:10.1016/j.jocn.2005.09.004

until analysis. Brain magnetic resonance imaging (MRI) studies of these seven patients were performed at the same time as the CSF collection and the results showed no brain atrophy in two, slight atrophy in three, and moderate atrophy in two patients. The CSF of the remaining four patients with definite CJD (patients 8 to 11; Table 1) was collected fresh in the terminal stages 1.5–4 years after onset and was stored at −80 °C until analysis. The brain MRI scans of these four patients showed very severe brain atrophy, very thin cortices and white matter, and enormously dilated ventricles. The profiles of the patients enrolled in this study, including the clinical, laboratory, and radiological findings, are listed in Table 1.

To detect 14-3-3 protein in CSF, we initially analysed the CSF using the polyclonal rabbit antibodies SC-629 (Santa Cruz Biotechnology, Santa Cruz, CA, USA), which react to the common epitopes of all 14-3-3 isoforms (pan 14-3-3). To verify the isoform specificities of the 14-3-3 antibodies, we evaluated the cross-reactivities of the antibodies we raised against each 14-3-3 isoform[9] and the commercially available antibodies by dot hybridisation as follows: six different recombinant isoforms (β, τ, η, ζ, ε, and γ; 10 ng) were dotted onto a nitrocellulose membrane and incubated with the antibodies against 14-3-3 isoforms (β, τ, η, ε, and γ). The commercially available antibodies SC-628 for 14-3-3 β, SC-732 for 14-3-3 τ, SC-1019 for 14-3-3 ζ, SC-1020 for 14-3-3 ε, and SC-731 for 14-3-3 γ (Santa Cruz Biotechnology, Santa Cruz, CA, USA) were also evaluated.

Twenty μL of each CSF specimen was subjected to 10–20% gradient sodium dodecyl sulfate–polyacrylamide gel electrophoresis (SDS-PAGE), and then transferred onto an Immobilon P membrane (Millipore, Fremont, CA, USA) at 90 mA for 120 min. The membranes were subsequently treated with 3% skim milk (Yukijirushi, Sapporo, Japan) for 1 h at room temperature, and then reacted with SC-629 pan 14-3-3 antibodies and the isoform-specific antibodies (2 μg/mL for SC-629, 14-3-3 γ, ε, η, β, and τ, and 0.2 μg/mL for SC-1019) at 4 °C overnight. The membranes were incubated with 1:5000 dilutions of horseradish peroxidase (HRP)-conjugated anti-rabbit immunoglobulin G (IgG; Zymed, South San Francisco, CA, USA) or 1:4000 dilutions of HRP-conjugated anti-mouse IgG (Dako, Carpinteria, CA, USA) for 1 h at room temperature. The immunoreactive bands were visualised on Fuji RX-U films (Fujifilm, Tokyo, Japan) using enhanced chemiluminescence (ECL) detection reagents (Amersham Pharmacia, Piscataway, NJ, USA). Recombinant proteins of each 14-3-3 isoform (0.63 to 10 ng) prepared as described elsewhere[9] were also subjected to SDS-PAGE and Western blotting as standards. After visualisation with ECL, the densities of the immunoreactive 14-3-3 peaks (optical density (OD) units) were measured with an NIH image analysing system 1.62 (National Institutes of Health, Bethesda, MD, USA) and the levels of total 14-3-3 protein were estimated from the standard curves for the same gel as reported elsewhere.[9]

In 11 patients, neuron-specific enolase (NSE) was measured commercially using an enzyme-linked immunosorbent assay kit (SRL laboratory, Tokyo, Japan) with the same CSF.

3. Results

In seven patients (patients 1 to 7) whose brain MRI scans were normal or showed moderate atrophy, we detected an immunoreactive 30-kDa band against SC-629 (Fig. 1A). In patients 1–6, who had a clear band corresponding to the 14-3-3 protein, the NSE value was more than 25 ng/mL, the cut-off value.[10] However, in patient 7, who had a weak band, the NSE value was 15.8 ng/mL. In the other four patients (patients 8 to 11), whose brain MRI scans indicated very severe brain atrophy, the band was not detected (Fig. 1A). The NSE values of these patients were less than 10 ng/mL. The levels of total 14-3-3 protein in the CSF determined by SC-629 were significantly

Table 1
Profiles of patients enrolled in this study

Patients	1	2	3	4	5	6	7	8	9	10	11
Age/Sex	66/F	74/F	71/M	67/F	55/F	75/F	70/F	79/M	72/F	71/M	74/M
Initial symptom	Head heaviness	Dementia	Dressing apraxia	Diplopia	Somnolence	Ataxia	Ataxia, dementia	Ataxia	General fatigue	Hearing loss	Hallucination
PRNP	ND	ND	M/M	ND	M232R	V/V	ND	V180I	ND	ND	M/M
Myoclonus	+	+	+	+	+	−	+	+	+	+	+
PSWC	+	+	+	+	+	−	+	−	+	+	+
NSE	300	72	25.2	95	110	48	15.8	<10	<10	<10	<10
14-3-3	+	+	+	+	+	+	+	−	−	−	−
Autopsy	ND	+	ND	ND	ND	+	ND	+	ND	ND	+
DL	P	D	P	P	P	D	P	D	P	P	D
Atrophy	Moderate	Slight	Slight	No	No	Slight	Moderate	Severe	Severe	Severe	Severe

F = female, M = Male, PRNP = human prion protein gene, ND = not done, M/M = methionine homozygosity at codon 129 of human prion protein gene, M232R = a point mutation (methionine to arginine) at codon 232 of human prion protein gene, V/V = valine homozygosity at codon 129 of human prion protein gene, V180I = a point mutation (valine to isolecine) at codon 180 of human prion protein gene, PSWC = periodic sharp wave complexes, NSE = neuron specific enolase in the cerebrospinal fluid (ng/mL), 14-3-3 = 14-3-3 protein in the cerebrospinal fluid; DL = diagnostic level based on WHO criteria; P = probable; D = definate; Atrophy = cerebral atrophy estimated by magnetic resonance imaging.

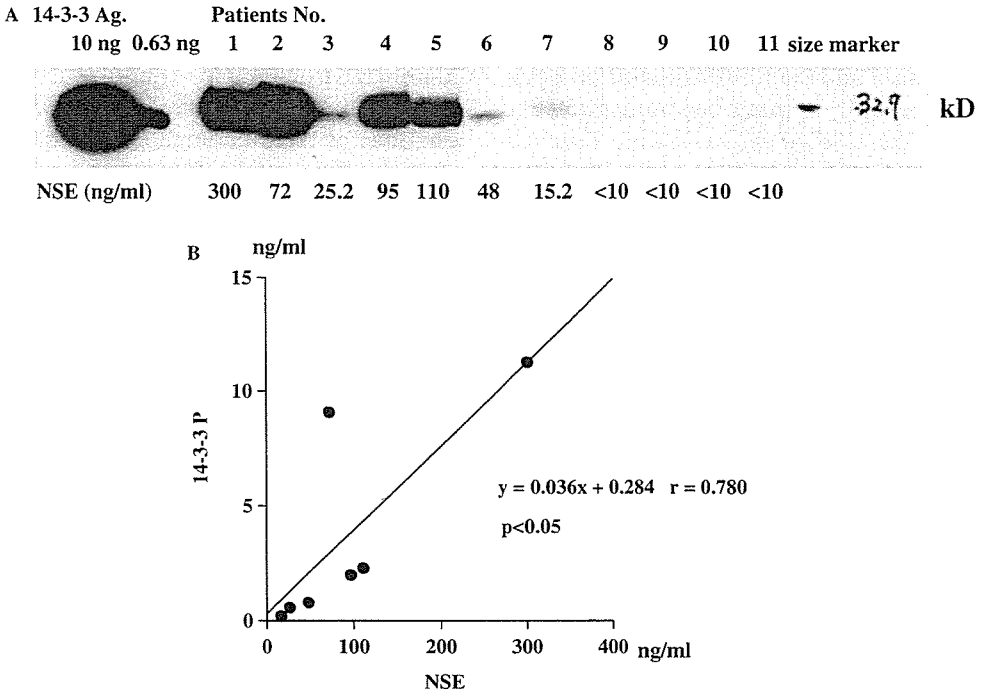

Fig. 1. Detection of 14-3-3 protein in the cerebrospinal fluid (CSF) of Creutzfeld-Jakob disease (CJD) patients. (A) Western immunoblotting analyses of total 14-3-3 protein in 11 CJD patients using SC-629 antibodies. The levels of neuron-specific enolase (NSE) of these patients were also measured by using an enzyme-linked immunosorbent assay kit. We detected 14-3-3 protein clearly in the CSF of patients 1–6, slightly in patient 7, and not at all in the CSF of patients 8–11. (B) Correlations between the levels of 14-3-3 and those of NSE. The 14-3-3 protein levels in the CSF correlated with those of NSE ($R = 0.780, p < 0.05$).

correlated with those of NSE (Fig. 1B). To analyse the isoform pattern of 14-3-3 in the CSF of the CJD patients, we then evaluated the cross-reactivities of the antibodies we raised and the commercial antibodies against the 14-3-3 isoforms as shown in Fig. 2. The monoclonal antibody for 14-3-3 τ, the polyclonal antibody for η that we raised, and SC-1019 for 14-3-3 ζ were highly specific. The polyclonal antibodies for 14-3-3 γ, ε, and β that we prepared were nearly specific except for a slight cross-reaction with 14-3-3 ζ, although commercially available SC-628, SC-732, SC-1020, and SC-731 showed lower isoform specificities (Fig. 2A,B). Based on these results, we analysed the isoform patterns of the CJD patients using the antibodies we prepared for 14-3-3 β, τ, η, ε, and γ, and the commercial SC-1019 for 14-3-3 ζ.

In the six definitely 14-3-3-positive patients (patients 1 to 6), we examined the 14-3-3 isoform patterns (Fig. 3). All patients had an immunoreactive band against 14-3-3 γ, ε, ζ, η and β, except for patients 3 and 6, who had a trace immunoreactive band against 14-3-3 η. However, the 14-3-3 τ isoform was not detected in these patients.

4. Discussion

In this study we found that: (1) 14-3-3 protein in the CSF was clearly detected in the progressive stages but

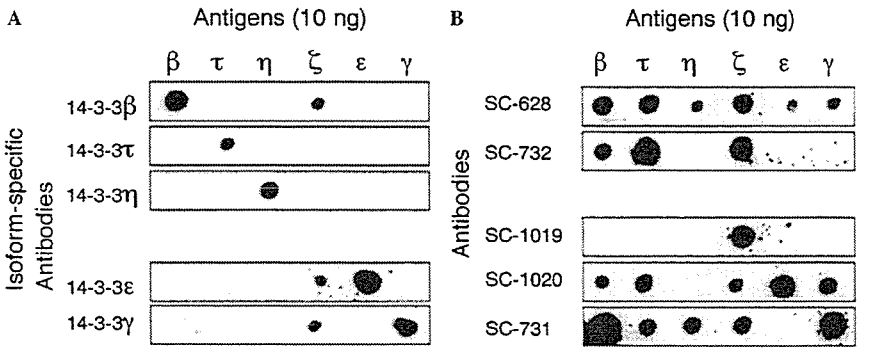

Fig. 2. Specificity of antibodies against 14-3-3 isoforms. (A) The antibodies we raised against 14-3-3 τ and η were highly specific, and those against 14-3-3 γ, ε, and β were nearly specific except for a slight cross-reaction with 14-3-3 ζ. These antibodies reacted at a concentration of 2 μg/mL. (B) Among the commercially available antibodies, SC-1019 was highly specific for 14-3-3 ζ, but SC-628, SC-732, SC-1020, and SC-731 demonstrated cross-reactivity with other isoforms. The antibodies reacted at a concentration of 0.2 μg/mL. All comercial antibodies from Santa Cruz Biotechnology, Santa Cruz, CA, USA.

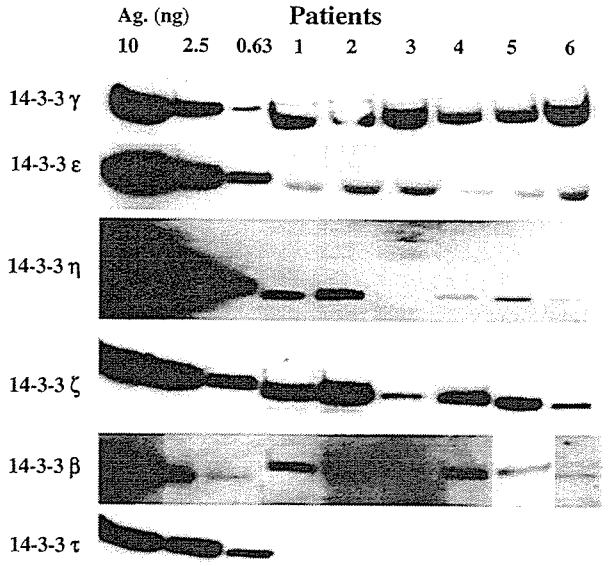

Fig. 3. 14-3-3 isoform patterns in the cerebrospinal fluid of Creutzfeld-Jakob disease (CJD) patients as detected by Western immunoblotting. The 14-3-3 isoforms of CJD patients 1–6 were detected by the isoform-specific antibodies in Fig. 2A and SC-1019 in Fig. 2B. Each recombinant 14-3-3 isoform protein (0.63–10 ng) was also used as a standard.

not in the terminal stages of the disease, when the brain was severely atrophied; (2) the detected 14-3-3 protein in the CSF of CJD patients comprised five brain-native isoforms; and (3) the levels of 14-3-3 protein in the CSF of CJD patients were correlated with those of NSE, which is a brain-specific protein. These findings reconfirm the fact that 14-3-3 protein is released into the CSF as a consequence of the extensive and rapid destruction of the brain. The detection of five 14-3-3 isoforms, γ, ε, η, ζ, and β, may enhance the diagnostic value of 14-3-3 protein in the CSF.

After it was reported that 14-3-3 protein in the CSF is useful for diagnosing CJD,[1] many neurologists studied the protein as a potentially specific marker of CJD. Although 14-3-3 protein is ubiquitously present in almost all tissues, it is particularly abundant in the brain, comprising approximately 1% of the total soluble protein in the brain.[11] 14-3-3 protein is essential for cells to survive and acts as an anti-apoptotic protein by regulating protein phosphorylation.[12] 14-3-3 protein with a positive NSE result[13] was detectable in the CSF in a relatively early phase of CJD, but was under the detection limit in the terminal stage when the brain was severely atrophied. These results suggest that, even in the CSF of typical CJD patients, 14-3-3 protein cannot be detected after neuronal loss is nearly complete. The positive rate of 63.6% (seven of 11) for the 14-3-3 protein immunoassay in the present study was lower than that found in another study.[14] We think the reason for this is that four patients in the terminal stage were included among our 11 patients, not because various subtypes of CJD were included.

In the isoform assay of the CJD patients, we detected five isoforms, 14-3-3 γ, ε, η, ζ, and β, but not the τ isoform (Fig. 3). 14-3-3 τ is restricted to the hippocampus and medulla oblongata of the mammalian brain, and it is present in very low amounts.[6] A pathological study showed that the hippocampus and medulla are relatively less affected in CJD, and that T lymphocytes, in which 14-3-3 τ is rich,[15] hardly invade or accumulate in the lesions.[16] These results may support the conclusion that 14-3-3 τ in CSF is under the detection limit. Previously, Van Everbroeck et al. described the detection of 14-3-3τ by using the antibody SC-732,[17] but this antibody reacts not only with τ but also with β and ζ, as shown in Fig. 2, suggesting that their result may reflect the cross-reaction of SC-732 with the 14-3-3 β and ζ isoforms. The isoform patterns of 14-3-3 protein in the CSF of CJD patients are controversial, and a consensus has not been established yet; γ isoforms,[1,18] ε and γ isoforms,[7] and β, γ, ε, and η isoforms,[8] partly consistent with our data, have been reported. Based on the results shown in Fig. 2, we speculate that inadequate isoform specificity of the antibodies used may be the cause of the differences in isoform patterns. The great improvements in terms of isoform specificity of the antibodies that we raised may provide more reliable results.

14-3-3 protein is not detected immunologically in the CSF of healthy humans and mammals, and its presence in the CSF suggests leakage of brain cellular proteins due to massive neuronal disruption.[19] Although the detection of 14-3-3 protein in CSF is a sensitive marker for CJD, positive detection has also been reported in other acutely destructive brain diseases, such as cerebrovascular disease, herpes simplex encephalitis, acquired immunodeficiency syndrome (AIDS), malignant brain tumor, hypoxic brain damage, and metabolic encephalopathy.[1,3,9] Although we did not study the CSF of normal controls because of ethical concerns, we previously reported analyses of 14-3-3 protein, including its isoform pattern, in the CSF of four patients with AIDS dementia complex (ADC), six with cytomegalovirus encephalitis (CMVE), six with cryptococcal meningoencephalitis (CCME), and eight control patients consisting of four with aseptic meningitis, two with amyotrophic lateral sclerosis, one with myasthenia gravis, and one with Parkinson's disease, using the same antibodies as those used in the present study.[9] The ε and γ isoforms were detected in CCME, the ε, γ, ζ, and β isoforms were detected in ADC, and the ε, γ, and ζ isoforms were detected in CMVE. However, 14-3-3 protein was not detected in the control patients.[9] The existence of five 14-3-3 isoforms, 14-3-3 γ, ε, η, ζ, and β, in the CSF is characteristic of CJD, and detecting the five isoforms is important for a diagnosis of CJD.

Although re-evaluation of the 14-3-3 isoform pattern by using isoform-specific antibodies may still be required, the technique may be useful to differentiate CJD from other diseases, including acutely progressive central nervous system disorders. In addition, the isoform pattern in CJD patients may reflect a difference in the 14-3-3 isoform distribution in the brain.[6]

Acknowledgement

We thank Mr. Brent Bell for reading the manuscript, Dr. Tetsuyuki Kitamoto for analysing the prion protein gene, and Drs Naoshi Okita and Sumireko Sekiguchi for their clinical support. Part of this work was presented at the 125th Annual Meeting of the American Neurological Association, Boston, MA, 17 October 2000. This work was supported by the Slow Virus Infection Research Committee, of the Ministry of Health, Labor and Welfare of Japan.

References

1. Zerr I, Bodemer M, Gefeller O, et al. Detection of 14-3-3 protein in the cerebrospinal fluid supports the diagnosis of Creutzfeldt-Jakob disease. *Ann Neurol* 1998;**43**:32–40.
2. Zeidler M, Gibbs Jr CJ, Meslin F. *WHO Manual for Strengthening Diagnosis and Surveillance of Creutzfeldt-Jakob Disease*. Geneva: WHO; 1998.
3. Huang N, Marie SK, Livramento JA, et al. 14-3-3 protein in the CSF of patients with rapidly progressive dementia. *Neurology* 2003;**61**: 354–7.
4. Chapman T, McKeel Jr DW, Morris JC. Misleading results with the 14-3-3 assay for the diagnosis of Creutzfeldt-Jakob disease. *Neurology* 2000;**55**:1396–7.
5. Leffers H, Madsen P, Rasmussen HH, et al. Molecular cloning and expression of the transformation sensitive epithelial marker stratifin. A member of a protein family that has been involved in the protein kinase C signalling pathway. *J Mol Biol* 1993;**20**:982–98.
6. Baxter HC, Liu WG, Forster JL, et al. Immunolocalisation of 14-3-3 isoforms in normal and scrapie-infected murine brain. *Neuroscience* 2002;**109**:5–14.
7. Takahashi H, Iwata T, Kitagawa Y, et al. Increased levels of ε and γ isoforms of 14-3-3 proteins in cerebrospinal fluid in patients with Creutzfeldt-Jakob disease. *Clin Diagn Lab Immunol* 1999;**6**:983–5.
8. Wiltfang J, Otto M, Baxter HC, et al. Isoform pattern of 14-3-3 proteins in the cerebrospinal fluid of patients with Creutzfeldt-Jakob disease. *J Neurochem* 1999;**73**:2485–90.
9. Wakabayashi H, Yano M, Tachikawa N, et al. Increased concentrations of 14-3-3 ε, γ and ζ isoforms in cerebrospinal fluid of AIDS patients with neuronal destruction. *Clinica Chimica Acta* 2001;**312**: 97–105.
10. Beaudry P, Cohen P, Brandel PJ, et al. 14-3-3 protein, neuron-specific enolase, and S-100 protein in cerebrospinal fluid of patients with Creutzfeldt-Jakob disease. *Dement Geriat Cogn Disord* 1999;**10**:40–6.
11. Boston PF, Jackson P, Thompson RJ. Human 14-3-3 protein: radioimmunoassay, tissue disturbance, and cerebrospinal fluid levels in patients with neurological disorders. *J Neurochem* 1982;**38**:1475–82.
12. Wang HG, Pathan N, Ethell IM, et al. Ca^{2+}-induced apoptosis through calcineurin dephosphorylation of BAD. *Science* 1999;**284**: 339–43.
13. Zerr I, Bodemer M, Räcker S, et al. Cerebrospinal fluid concentration of neuron-specific enolase in diagnosis of Creutzfeldt-Jakob disease. *Lancet* 1995;**345**:1609–10.
14. Shiga Y, Miyazawa K, Sato S, et al. Diffusion-weighted MRI abnormalities as an early diagnostic marker for Creutzfeldt-Jakob disease. *Neurology* 2004;**63**:443–9.
15. Meller N, Liu YC, Collins TL, et al. Direct interaction between protein kinase CθPKCθ and 14-3-3 t in T cells: 14-3-3 overexpression results in inhibition of PKCθ translocation and function. *Mol Cell Biol* 1996;**16**:5782–91.
16. Sánchez-Valle R, Saiz A, Graus F. 14-3-3 protein isoforms and atypical patterns of the 14-3-3 assay in the diagnosis of Creutzfeldt-Jakob disease. *Neurosci Lett* 2002;**320**:69–72.
17. Van Everbroeck BRJ, Boons J, Cras P. 14-3-3 γ-isoform detection distinguishes sporadic Creutzfeldt-Jakob disease from other dementias. *J Neurol Neurosurg Psychiatry* 2005;**76**:100–2.
18. Hsich G, Kenney K, Gibbs CJ, et al. The 14-3-3 brain protein in cerebrospinal fluid as a marker for transmissible spongiform encephalopathies. *N Engl J Med* 1996;**335**:924–30.
19. Lemstra AW, van Meegen MT, Vreyling JP, et al. 14-3-3 testing in diagnosing Creutzfeldt-Jakob disease: a prospective study in 112 patients. *Neurology* 2000;**55**:514–6.

Available online at www.sciencedirect.com
SCIENCE DIRECT
Vaccine 24 (2006) 2815–2823
Vaccine
www.elsevier.com/locate/vaccine

Enhanced mucosal immunogenicity of prion protein following fusion with B subunit of *Escherichia coli* heat-labile enterotoxin

Hitoki Yamanaka [a], Daisuke Ishibashi [a], Naohiro Yamaguchi [b], Daisuke Yoshikawa [b], Risa Nakamura [b], Nobuhiko Okimura [b], Takeshi Arakawa [c], Takao Tsuji [d], Shigeru Katamine [b], Suehiro Sakaguchi [a,b,*]

[a] *PRESTO Japan Science and Technology Agency, 4-1-8 Honcho Kawaguchi, Saitama, Japan*
[b] *Department of Molecular Microbiology and Immunology, Nagasaki University Graduate School of Biomedical Sciences, 1-12-4 Sakamoto, Nagasaki 852-8523, Japan*
[c] *Division of Molecular Microbiology, Center of Molecular Biosciences, University of the Ryukyus, 1 Senbaru, Nishihara, Okinawa 903-0213, Japan*
[d] *Department of Microbiology, Fujita Health University School of Medicine, Toyoake, Aichi 470-1192, Japan*

Received 12 May 2005; received in revised form 10 December 2005; accepted 27 December 2005
Available online 17 January 2006

Abstract

Mucosal vaccine against prion protein (PrP), a major component of prions, is urgently awaited since the oral transmission of prions from cattle to humans is highly suspected. In the present study, we produced recombinant bovine and mouse PrPs fused with or without the B subunit of *Escherichia coli* heat-labile enterotoxin (LTB) and intranasally immunized mice with these fused proteins. Fusion with LTB markedly enhanced the mucosal immunogenicity of bovine PrP, producing a marked increase in specific IgG and IgA titer in serum. Mouse PrP also showed slightly increased immunogenicity following fusion with LTB. These results demonstrate that LTB-fused PrPs might be potential candidates for protective mucosal prion vaccines.

Keywords: Prion; Mucosal vaccine; Heat-labile enterotoxin

1. Introduction

Prion diseases including Creutzfeldt-Jakob disease (CJD) in humans, bovine spongiform encephalopathy (BSE) in cattle and scrapie in sheep are devastating neurodegenerative disorders [1,2]. Most cases of CJD are sporadic with unknown etiologies [3]. About 10% of CJD cases are inherited diseases associated with mutations of the prion protein (PrP) gene [3], and most of the remaining cases were iatrogenically transmitted via prion-contaminated electroencephalogram electrodes, human growth hormone preparations, dura matter and corneal grafts [4–7]. Recent lines of evidence indicate that BSE prions could be orally transmitted to humans via contaminated food, causing more than 100 cases of a new variant (nv) CJD in young people, especially in England [8,9]. It is therefore of great importance to develop prion vaccines, in particular those enhancing mucosal immunity, to prevent oral transmission of prions, such as from cattle to humans.

Prions are thought to be mainly composed of the proteinase K (PK)-resistant, amyloidgenic isoform of PrP, designated PrP^{Sc} [10]. PrP^{Sc} is generated by the conformational conversion of the normal isoform of PrP, PrP^{C}, a glycosylphosphatidylinositol-anchored membrane glycoprotein abundantly expressed in neurons [10]. Gabizon et al.

* Corresponding author at: Department of Molecular Microbiology and Immunology, Nagasaki University Graduate School of Biomedical Sciences, 1-12-4 Sakamoto, Nagasaki 852-8523, Japan. Tel.: +81 95 849 7059; fax: +81 95 849 7060.
E-mail address: suehiros-ngs@umin.ac.jp (S. Sakaguchi).

0264-410X/$ – see front matter © 2006 Elsevier Ltd. All rights reserved.
doi:10.1016/j.vaccine.2005.12.054

previously reported that polyclonal antibodies against PrP could reduce the infectivity of hamster-adapted scrapie prions [11]. Heppner et al. also recently showed that mice transgenically expressing anti-PrP monoclonal antibody, 6H4, were resistant to the disease after intraperitoneal inoculation of mouse-adapted scrapie RML prions [12]. It was further reported that passive immunization with two other anti-PrP monoclonal antibodies, ICSM 18 and 35, could protect mice from prion infection [13]. Such successful prevention of the prion infection by anti-PrP antibodies indicates that mucosal vaccination against PrP could be a more rational way to block the oral transmission of prions. However, the host is already immunologically tolerant to PrP, hampering the development of prion vaccines.

Escherichia coli heat-labile enterotoxin (LT) and cholera toxin (CT) are highly potent adjuvants for mucosal immunity [14,15]. The mechanism of how these toxins elicit mucosal immunity is not fully understood. These toxins consist of one A subunit and a pentamer of B subunits [14,15]. The A subunit carries enzymatic activity and the B subunit pentamer mediates binding of the toxins to GM_1 gangliosides on target epithelial cells [14,15]. Upon binding of these toxins to cells, the A subunit enters the cells and exerts its toxicity via ADP-ribosylation of adenylate cyclase [14,15]. The B subunit of LT (LTB) or CT (CTB) is a strong modulator of mucosal immunity and fusion with these B subunits could enhance the mucosal immunogenicity of certain peptides [14,15].

In the present study, we successfully demonstrate for the first time that fusion with LTB markedly enhanced the mucosal immunogenicity of bovine (bo) PrP to elicit strong antibody responses in mice. Slightly increased responses could also be observed against mouse (mo) PrP fused with LTB in mice.

2. Materials and methods

2.1. Plasmid construction and purification of recombinant PrPs

2.1.1. LTB-moPrP120-231 and LTB-boPrP132-242

The DNA fragment for LTB residues 22–124 (*E. coli* MV1184) with sequences for the *Eco*RV site at the 5′-terminus and for the Gly-Pro-Gly-Pro and *Eco*RI site at the 3′-terminus was amplified by polymerase chain reaction (PCR). The fragment for moPrP residues 120–231 (GenBank accession no. M13685) and boPrP residues 132–242 (D10612) containing the *Eco*RI site at the 5′-terminus and the *Xho*I site at the 3′-terminus, were similarly amplified by PCR. Following sequence confirmation of these PCR products, the LTB and PrP fragments were digested and simultaneously inserted into a pET20b(+) vector (Novagen Inc., WI, USA), resulting in pET-LTB-moPrP120–231 and pET-LTB-boPrP132–242. *E. coli* (BL21) cells being transformed by these plasmids and cultured in LB medium. The recombinant proteins were expressed by 1 mM isopropyl β-D-thiogalactoside (IPTG). The cells were collected by centrifugation, lysed using CelLytic B Bacterial Cell Lysis/Extraction Reagent (Sigma–Aldrich Co., St Louis, USA) in the presence of DNase I, and centrifuged at 25,000 × *g* for 10 min. The resulting supernatant was purified using a Ni-NTA column (Qiagen, Hilden, Germany) under native conditions as recommended in the manufacturer's protocol.

2.1.2. moPrP120–231 and boPrP132–242

The DNA fragments encompassing moPrP residues 120–231 and boPrP residues 132–242 were amplified by PCR. The *Bam*HI and *Hin*dIII sites were introduced at the 5′- and 3′-termini of these fragments, respectively. These fragments were then digested and inserted into a pQE30 vector (Qiagen), resulting in pQE30-moPrP120–231 and pQE30-boPrP132–242. *E. coli* (M15) cells were transformed by these plasmids and cultured in LB medium containing 1 mM IPTG. The cells were collected by centrifugation, suspended in PBS containing 2% Triton X-100, and lysed by ultrasonication. This lysate was centrifuged at 35,000 × *g* for 15 min. The resulting pellet was resolved in PBS containing 8 M urea and 20 mM 2-mercaptoethanol and applied to a Ni-NTA column (Qiagen). The proteins were finally eluted with PBS containing 500 mM imidazole.

2.1.3. moPrP23–231 without a 6 × His tag

The DNA fragment for moPrP residues 23–231 with the *Nde*I site at the 5′-terminus and the *Bam*HI site at the 3′-terminus were amplified by PCR. The fragment was digested and inserted into pET11a (Novagen), resulting in pET11a-moPrP23–231. *E. coli* (BL21) cells were transformed with the plasmid and cultured in LB medium containing 1 mM IPTG. The cells were collected by centrifugation and resuspended in a buffer (50 mM Tris–HCl, pH 8, 1 mM EDTA, 100 mM NaCl, 1 mM PMSF) containing 300 μg/ml lysozyme, deoxycholic acid and DNase I. The resulting extract was centrifuged at 25,000 × *g* for 20 min and the pellet was solubilized in a buffer (8 M urea, 50 mM Tris–HCl, 1 mM EDTA, pH 8). This extract was applied to a CM-sepharose column (Amersham Pharmacia Biotech AB, Uppsala, Sweden) and recombinant PrP was eluted using a linear NaCl gradient from 0 to 500 mM.

2.2. GM_1 ganglioside binding assay

A 96 well immunoplate (Nunc, Roskilde, Denmark) was coated with 200 ng of GM_1 ganglioside (Sigma–Aldrich Co.) in a 50 mM carbonate buffer (pH 9.6) and blocked with PBS containing 0.05% Tween-20 and 25% Block Ace (Dainihonseiyaku Co., Tokyo, Japan). The fusion proteins were incubated in the wells for 1 h at 37 °C. Binding of the proteins to GM_1 ganglioside was visualized using anti-LT mouse serum raised against recombinant LT and anti-mouse IgG antibodies conjugated with horseradish peroxidase (HRP, Amersham Biosciences, NJ, USA).

2.3. Nasal immunization of mice with PrPs

Purified proteins were dialyzed against PBS and 10 μl containing 10 μg proteins and 1 μg of an adjuvant mutant LT were administered into each external nare of female 8-week-old C57BL/6 and Balb/c mice (SLC Japan, Shizuoka, Japan) at 2-week intervals. Mutant LT toxin lacking residues Arg192, Thr193 and Ile194 in the A subunit was prepared as previously described [16]. Mice were cared for in accordance with the Guidelines for Animal Experimentation of Nagasaki University.

2.4. Determination of specific IgG and IgA antibody titers

Each well of a 96 well immunoplate (Nunc) was coated with 500 ng of purified moPrP without a 6 × His tag or 6 × His-tagged boPrP by overnight incubation at 4 °C and then blocked with PBS containing 0.05% Tween-20 (T-PBS) and 25% Block Ace (Dainihonseiyaku Co.) at 37 °C for 1 h. To detect anti-boPrP or anti-moPrP antibodies, serially 10- or 8-fold diluted antiserum was added to the wells for 1 h at 37 °C, respectively, and unbound antibodies were removed by washing twice with T-PBS. Immune complexes were detected using secondary goat anti-mouse IgA (Sigma) or sheep anti-mouse IgG antibodies conjugated with HRP (Amersham Biosciences).

2.5. Quantification of anti-PrP IgA in fecal extract

Each well of a 96 well immunoplate (Nunc) was coated with 500 ng of purified 6 × His-tagged boPrP by overnight incubation at 4 °C and then blocked with PBS containing 0.05% Tween-20 (T-PBS) and 25% Block Ace (Dainihonseiyaku Co.) at RT for 1 h. The fecal extracts were prepared according to a manufacturer's protocol. In brief, ~30 mg of feces were homogenized in 600 μl of PBS containing a protease inhibitor cocktail (Nacalai Tesque Inc., Kyoto, Japan) and centrifuged to remove insoluble materials. Two-fold diluted supernatant of the fecal extract was added to the wells for 1 h at RT and unbound antibodies were removed by washing twice with T-PBS. Immune complexes were detected using secondary goat anti-mouse IgA antibody conjugated with HRP (Amersham Biosciences). The concentration of specific IgA in the fecal extract was determined from a standard curve plotted using an already-known standard concentration of IgA (BETHYL Lab. Inc., Texas, USA).

2.6. Transfection

African green monkey kidney COS-7 cells were cultured in Dulbecco's modified Eagle medium (Invitrogen, Carlsbad, CA) containing 10% fetal bovine serum and transfected by a pcDNA3.1 vector (Invitrogen) inserted with or without the cDNA encoding bo, sheep (sh), and human (hu) PrP^C using lipofectamin 2000 (Invitrogen). These cells were then subjected to immunoblotting or FACS analysis 3 days after transfection.

2.7. Immunoblotting

COS-7 cells were lysed in buffer (1% Triton X-100, 1% sodium deoxycholate, 300 mM NaCl, 100 mM Tris–HCl, pH 7.5) and brain tissues were homogenized in PBS. Thirty micrograms of total proteins were treated with or without 20 μg/ml proteinase K for 30 min at 37 °C, electrophoresed on a 12% SDS-polyacrylamide gel, and electrically transferred onto a nitrocellulose membrane (Millipore, MA, USA). The membrane was incubated with antiserum for 2 h. The signals were visualized using HRP-conjugated secondary anti-mouse IgG antibodies and the ECL system (Amersham Biosciences).

2.8. FACS

Cells were harvested with PBS containing 0.2% EDTA, suspended in BSS buffer (140 mM NaCl, 5.4 mM KCl, 0.8 mM $MgSO_4$, 0.3 mM Na_2HPO_4, 0.4 mM KH_2PO_4, 1 mM $CaCl_2$), and incubated with 100-fold diluted antisera for 30 min on ice. The treated cells were then washed three times with BSS buffer, reacted with FITC-conjugated goat anti-mouse IgG (H + L) (Chemicon International, CA, USA), and analyzed by FACScan (Becton Dickinson, New Jersey, USA).

3. Results

3.1. Purification and characterization of LTB-fused mo and boPrPs

Since the C-terminal half of moPrP was shown to be recombinantly expressed in large amounts of soluble protein in the periplasmic space of *E. coli*. [17] and include the epitopes for anti-mouse prion antibodies [12,13], we constructed LTB-moPrP120–231 fusion protein by linking the C-terminal residues 120–231 of moPrP to the C-terminus of LTB with the hinge sequence Gly-Pro-Gly-Pro (Fig. 1a). LTB-boPrP132–242 was similarly constructed by fusion of boPrP residues 132–242 with LTB (Fig. 1a). These fusion proteins contain the signal peptide at the N-terminus to be secreted into the periplasmic space and a 6 × His sequence at the C-terminus allowing easy purification using a Ni-NTA column.

We partially purified these recombinant proteins in a soluble form. Coomassie brilliant blue staining of denatured LTB-moPrP120–231 and LTB-boPrP132–242 showed one major band with a molecular weight of ~25 kDa, corresponding to the monomeric fusion protein (Fig. 1b). In contrast, under non-denaturing electrophoresis conditions, these bands disappeared and were shifted to higher molecular weight ladder bands including one major band (Fig. 1b). The molecular

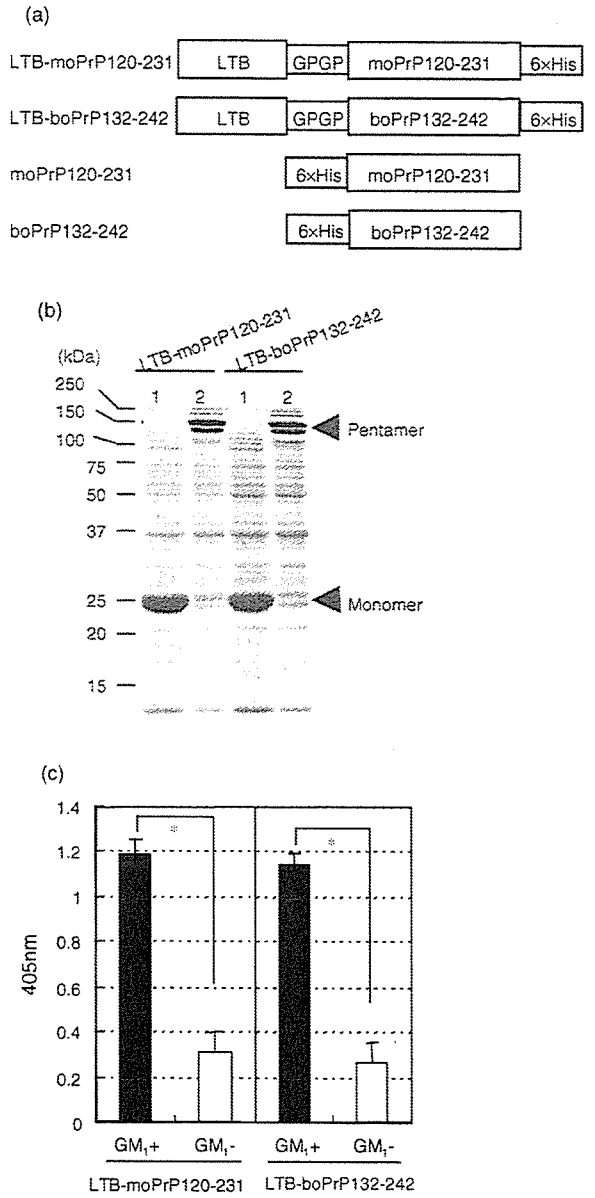

Fig. 1. Structural diagrams of mouse (mo) and bovine (bo) PrPs fused with or without LTB (a) and biochemical properties of LTB-fused PrPs (b and c). (b) LTB-moPrP120–231 and LTB-boPrP132–242 were boiled at 100 °C in denatured conditions and then electrophoresed on a 12% SDS-PAGE (lane no. 1). These denatured fusion proteins were monomeric. In contrast, without boiling (lane no. 2), the fusion proteins formed a pentameric structure. (c) LTB-moPrP120–231 and LTB-boPrP132–242 similarly bound to GM_1 ganglioside. The signals were expressed as colorimetric values measured at 405 nm. Four independent data from each group were analyzed using the Mann–Whitney *U*-test. Data were represented by mean ± standard deviation (S.D.). $^{*}p < 0.05$.

weight of these bands indicates that fusion proteins are at least pentameric in a native form.

We also examined whether these fusion proteins could bind to GM_1 ganglioside. The fusion proteins were first incubated on plates with or without immobilized GM_1 ganglioside and then colorimetrically detected by anti-LT antibodies. The colorimetric values obtained from complexes of fusion proteins bound to GM_1 ganglioside were significantly much higher than those of the fusion protein alone (Fig. 1c). Anti-PrP polyclonal antibodies also showed similar binding of the fusion proteins to GM_1 ganglioside (data not shown). These results thus indicate that the fusion proteins have conserved binding competence to GM_1 ganglioside.

3.2. Enhancement of mucosal immunogenicity of boPrP132–242 by fusion to LTB

To examine the effect of fusion with LTB on the mucosal immunogenicity of boPrP132–242, we intranasally immunized C57BL/6 and Balb/c mice with LTB-boPrP132–242 as well as non-fused boPrP132–242 as a control three times at 2-week intervals in the presence of recombinant mutant LT as an adjuvant. BoPrP132–242 was N-terminally tagged with a 6 × His sequence (Fig. 1a) and purified using a Ni-NTA column. Antisera were collected from these mice 1 week after the final immunization and subjected to ELISA against recombinant boPrP with a 6 × His tag to determine specific IgG and IgA antibody titers. BoPrP132–242 itself elicited a moderate IgG antibody response in Balb/c mice but not in C57BL/6 mice (Fig. 2a). No efficient IgA response against boPrP132–242 could be detected in either mouse strain (Fig. 2a). In contrast, LTB-boPrP132–242 markedly enhanced the immunogenicity in both mouse strains, producing an enhanced increase in anti-boPrP IgG and IgA titers in serum, except for IgA in C57BL/6 mice (Fig. 2a). A large amount of specific secretory IgA was consistently detected in the feces of LTB-boPrP132–242-immunized Balb/c mice (Fig. 2b).

3.3. Detection of native PrP^C and PrP^{Sc} by anti-LTB-boPrP132–242 serum

To examine whether the anti-LTB-boPrP132–242 sera could recognize native PrP^C, we first performed Western blotting of the COS-7 cell lysates expressing non-6 × His-tagged bo, sheep (sh), and human (hu) PrP^C with the antisera from the immunized Balb/c mice. No specific signals could be detected in the cells transfected with a control vector (Fig. 3a). $MoPrP^C$ could not be detected with the antisera (data not shown). In contrast, the antisera strongly reacted with bo and $shPrP^C$ and weakly with $huPrP^C$ (Fig. 3a). We next carried out FACS analysis of these cells with the antisera. Vector alone-transfected cells showed no signals (Fig. 3b). In contrast, a large number of the cells expressing bo, sh and $huPrP^C$ could be stained (Fig. 3b). These results indicate that LTB-boPrP132–242 could induce antibodies recognizing native PrP^C from a broad range of species.

We also performed Western blotting of the brains of normal and BSE-affected cattle as well as those of scrapie-affected sheep with the anti-LTB-boPrP132–242 serum. In the normal cattle, specific signals could be detected only in

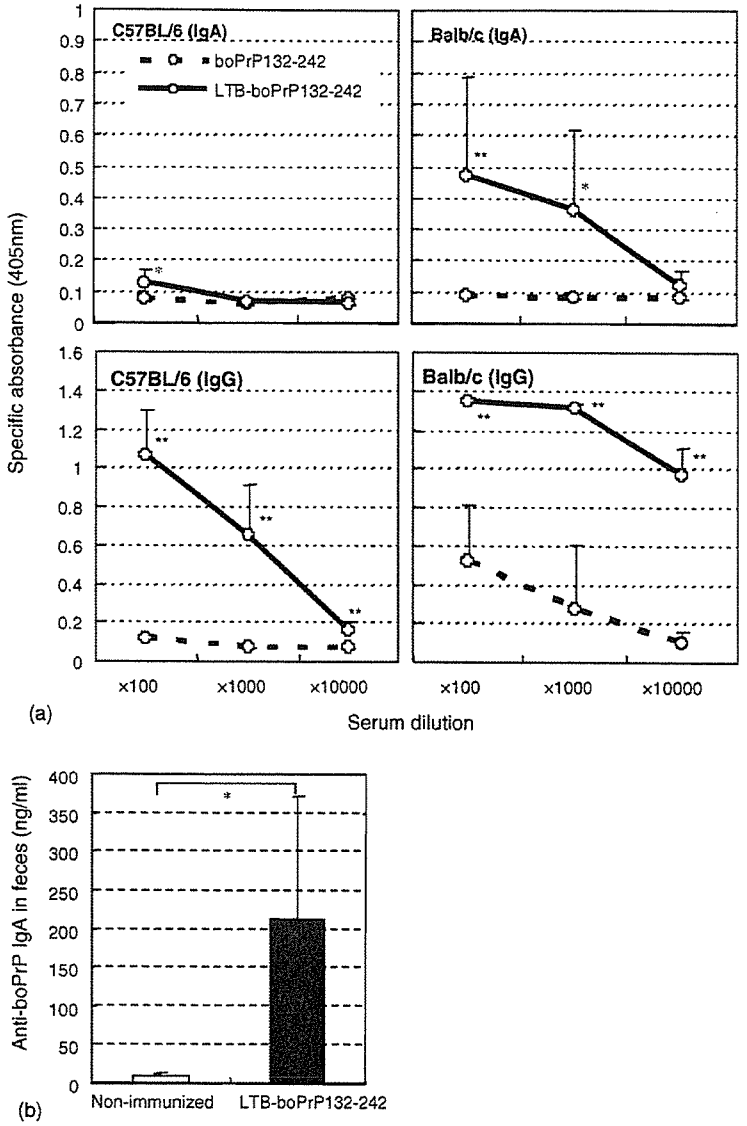

Fig. 2. (a) Specific IgA and IgG antibody titers in the serum of C57Bl/6 and Balb/c mice intranasally immunized with LTB-boPrP132–242 or boPrP132–242 three times at 2-week intervals. Antisera were collected from five mice from each group and were subjected to ELISA against 6 × His-tagged boPrP. Antibody titers were expressed by colorimetric values at 405 nm. (b) Amounts of specific IgA secreted in the feces of mice intranasally immunized with LTB-boPrP132–242 six times at 2-week intervals. Data were analyzed using the Mann–Whitney *U*-test. Data were represented by mean ± S.D. $^{*}p<0.05$; $^{**}p<0.01$.

the samples treated without PK (Fig. 3c), indicating that this antiserum could recognize $boPrP^{C}$ in normal cattle brains. Moreover, this antiserum could detect bo and $shPrP^{Sc}$ accumulated in the brains of BSE-cattle and scrapie-sheep, respectively (Fig. 3c).

3.4. Anti-LTB-boPrP132–242 antibodies recognize a potential anti-BSE prion epitope

Protective monoclonal antibodies, ICSN 35, 6H4 and ICSN 18, were shown to bind to moPrP residues 91–110, 144–152 and 146–159, respectively [12,13]. In addition, R1 and R2 Fab fragments bind to moPrP residues 220–231 and inhibit the accumulation of PrP^{Sc} in mouse neuroblastoma N2a cells infected with a prion [18]. These results strongly suggest that the corresponding regions in other PrPs are also potential anti-prion epitopes. To examine whether the antibodies against LTB-boPrP132–242 could react with these epitopes, we expressed the corresponding regions, boPrP residues 94–121, 143–166 and 231–242, as a fusion protein with glutathione *S*-transferase (GST) and subjected these proteins to Western blotting with the antisera. GST alone and GST-boPrP 94–121 and 231–242 could not be detected with the sera (Fig. 3d). However, GST-boPrP

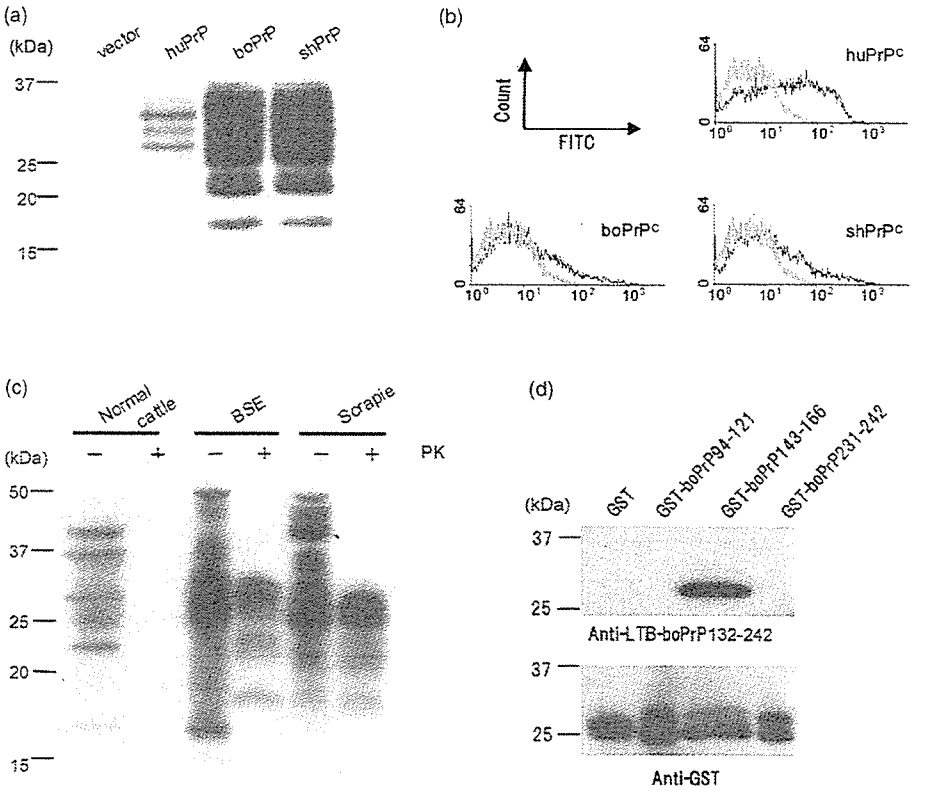

Fig. 3. Immunoblotting (a) and FACS analysis (b) of COS-7 cells expressing hu, bo, and shPrP^C with anti-LTB-boPrP132–242 sera. In (b), solid and gray lines indicate the cells transfected by a vector inserted with or without PrP cDNA, respectively. (c) Immunoblotting of the brains of normal and BSE-affected cattle and scrapie-affected sheep with anti-LTB-boPrP132–242 sera with (+) or without (−) treatment with proteinase K (PK). (d) Immunoblotting of GST-fused peptides of boPrP with anti-LTB-boPrP132–242 sera.

143–166 was substantially recognized with the sera (Fig. 3d), suggesting that immunization with LTB-boPrP132–242 could be prophylactic against BSE prions.

3.5. Anti-PrP autoantibodies in mice immunized with LTB-moPrP120–231 and LTB-boPrP132–242

To detect anti-moPrP IgG autoantibodies in Balb/c mice immunized with LTB-moPrP120–231 and LTB-boPrP132–242, we performed ELISA with these antisera against recombinant moPrP without a 6 × His tag. Mice were immunized six times at 2-week intervals. The mice immunized with moPrP120–231 could not elicit anti-PrP autoantibodies (Fig. 4a). However, immunization of mice with LTB-moPrP120–231 produced low but significantly higher titers of antibodies reactive with moPrP (Fig. 4a), indicating that fusion with LTB could break the tolerance of PrP only with very low efficiency. Similar or slightly lesser amounts of IgG cross-reactive with moPrP were observed in the mice immunized with boPrP132–242 but the fusion with LTB could not increase titers of the antibodies (Fig. 4b). Presumably due to low titers of the autoantibodies, we could not detect any specific reduction of PrP^{Sc} in the infected N2a cells treated with these antisera (data not shown).

4. Discussion

In the present study, we showed that fusion with LTB could markedly enhance the mucosal immunogenicity of boPrP132–242 in mice. Intranasal immunization with non-fused boPrP132–242 stimulated moderate antibody responses in Balb/c but not C57BL/6 mice. However, LTB-boPrP132–242 elicited very strong responses in both mouse strains, producing a marked increase in boPrP-specific IgA and IgG in serum. Specific secretory IgA was also abundantly observed in the intestines of the immunized mice.

The exact route of the orally ingested prions from the intestinal tract to the central nervous system is still uncertain. Accumulating evidence suggests that the ingested prions are transepithelially transported via M cells lining the intestinal membrane of Peyer's patches to the underlying follicular dendritic cells that are crucial for the prions to replicate and to reach the nervous system [19,20]. It was previously shown that certain monoclonal antibodies against PrP effectively prevented the infection of peripherally inoculated prions in mice, indicating that anti-PrP antibodies could neutralize prions invading the body [11–13]. IgA is a key player in pathogen-specific mucosal immunity. It is therefore feasible that anti-PrP IgA antibodies block the entry of

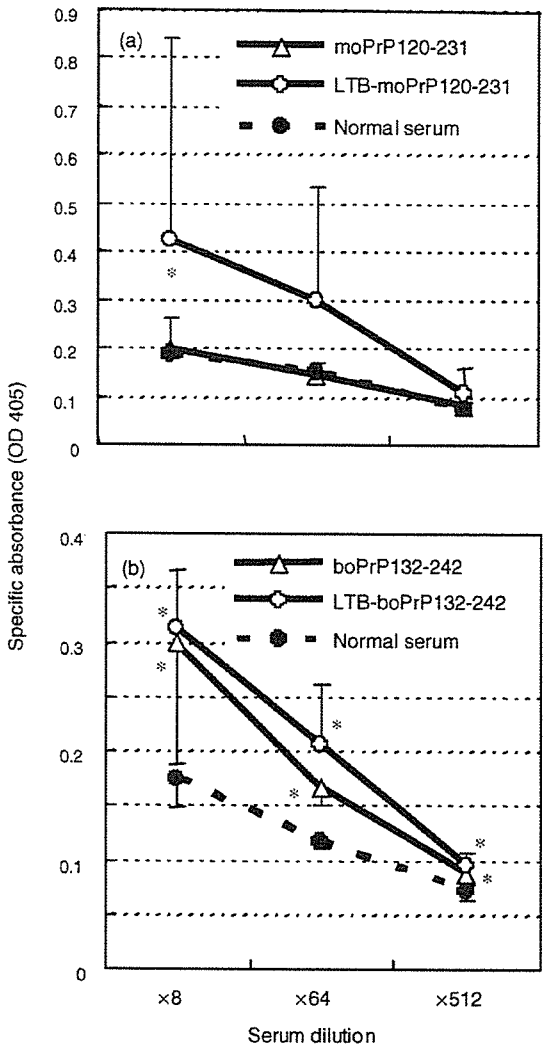

Fig. 4. Anti-moPrP autoantibodies in Balb/c mice immunized with mo (a) and boPrPs (b) fused with or without LTB, six times at 2-week intervals. Antisera were collected from four to five mice from each group and subjected to ELISA against moPrP without a 6 × His tag. Antibodies titers were expressed by colorimetric values at 405 nm. Data were analyzed using the Mann–Whitney *U*-test. Data were represented by mean ± S.D. $^{*}p < 0.05$.

orally ingested prions into the body. Intranasal immunization of mice with LTB-boPrP132–242 produced markedly higher titers of boPrP-specific IgG and IgA in sera irrespective of mouse strain genetic differences. We showed that the IgG antibodies could react with the putative anti-BSE prion epitope, strongly suggesting that these antibodies could neutralize BSE prions invading the body. We also showed that specific IgA was abundantly secreted in the intestines of these mice. It is therefore conceivable that orally-ingested BSE prions could be blocked at the intestinal entry point. Taken together, these results suggest that LTB-boPrP132–242 could be potent mucosal vaccines to prevent the transmission of prions from cattle to humans.

However, in nvCJD, the invading BSE prions convert endogenous human PrP^{C} into PrP^{Sc} upon the heterologous interaction with bovine PrP^{Sc}, and once human PrP^{Sc} is generated, the conversion effectively takes place via the syngeneic interaction of human PrP^{C} and human PrP^{Sc}. This constitutive syngeneic conversion of PrP results in fatal progression of the disease. To block the disease progression or to cure the disease, it is important to prevent the syngeneic interaction of human PrPs. Thus, boPrP-specific antibodies raised by LTB-boPrP132–242 vaccination probably have no therapeutic potential.

The prevalence of BSE within cattle is thought to be attributable to ingestion of BSE prion-contaminated food [21]. It is also recently reported that blood transfusion might be a risk factor for prion transmission in humans [22,23]. These urge the development of prophylactic measures against the intraspecies transmission of prions as well. However, individuals are tolerant to self-PrP. In fact, moPrP120–231 could barely evoke antibody responses in mice. However, fusion with LTB slightly but significantly induced IgG autoantibodies to moPrP in Balb/c mice, indicating that the fusion with LTB could circumvent the tolerance of PrP with very low efficiency. Intriguingly, immunization of mice with boPrP132–242 itself generated antibodies cross-reactive with moPrP with similar or slightly lower titers compared with those in LTB-moPrP120–231-immunized mice. In contrast to the case of moPrP120–231, fusion of boPrP132–242 with LTB could not enhance the production of cross-reactive antibodies in mice. These results suggest that immunization with heterologous recombinant PrPs themselves elicit autoantibodies in mice. It is therefore interesting to investigate whether or not immunization of mice with LTB-boPrP132–242 could be effective against the infections of mouse-adapted prions. If so, LTB-fused heterologous PrPs could be potential mucosal vaccines prophylactic against both the interspecies and the intraspecies transmission of prions.

Titers of the cross-reactive antibodies were very low in the mice immunized with LTB-fused boPrP132–242. Therefore, for vaccination with LTB-boPrP132–242 to be more effectively protective against the prion infection, it may be necessary to overcome B cell tolerance more efficiently. It was recently reported that oral vaccination with an attenuated *Salmonella typhimurium* strain expressing moPrP alone significantly delayed the disease in mice after inoculation of the mouse-adapted 139A scrapie prion, probably by eliciting autoantibodies against moPrP [24]. We showed here that mucosal vaccination of mice with LTB-fused moPrP120–231 or heterologous boPrP132–242 alone stimulated more production of anti-PrP autoantibodies than that of moPrP120–231 alone. It is therefore worthy to examine whether or not an attenuated *Salmonella typhimurium* strain expressing LTB-moPrP or heterologous PrPs could be more effective against the prion infection than one expressing moPrP alone. Molecular mimicry is a hypothetical mechanism for autoimmune diseases [25,26]. This hypothesis

postulates that shared identical amino acid sequences or homologous but non-identical amino acid sequences between microbial and host antigens could be essential for the initial processes of molecular mimicry, producing autoantibodies and/or auto-reactive T cells against the host antigens. Our results showing that heterologous boPrP was immunogenic inducing anti-PrP autoantibodies might be consistent with this hypothesis. Therefore, isolating molecules or peptides with much stronger antigenic mimicry to moPrP could be potentially important for prion vaccine development. It was reported that co-administration of moPrP with CpG-rich oligonucleotides, fusion of PrP with the heat shock protein DnaK, and dimerization of moPrP could break the tolerance and efficiently elicit autoantibodies against moPrP without inducing any autoimmune disease-specific symptoms in mice [27–29]. It is therefore interesting to investigate whether LTB-fused PrPs could increase the production of such cross-reactive antibodies either by co-administration with CpG or by such modifications of PrP. Nikes et al. recently showed that retrovirus-like particles (VLP) displaying the C-terminal 111 amino acids of moPrP fused with the transmembrane domain of the platelet-derived growth factor receptor could overcome B cell tolerance in mice to elicit anti-PrP autoantibodies able to react with native $moPrP^C$ [30]. It might also be interesting to investigate the immunogenicity of VPL displaying heterologous PrPs alone or LTB-fused heterologous PrPs. So far, no prion vaccines completely protective against prion infection have been developed. Further studies are required to determine how to circumvent B cell tolerance against PrP and induce much more antibodies protective against prion diseases.

Acknowledgements

We all thank Prof. Motohiro Horiuchi (Hokkaido University) for providing bovine PrP cDNA and brain tissues from BSE-affected cattle and scrapie-affected sheep. This study was supported in part by a Research on Specific Diseases grant from the Ministry of Health, Labour and Welfare, Japan.

References

[1] Prusiner SB. Prions. Proc Natl Acad Sci USA 1998;95:13363–83.
[2] Weissmann C, Enari M, Klohn PC, Rossi D, Flechsig E. Molecular biology of prions. Acta Neurobiol Exp (Wars) 2002;62:153–66.
[3] Will RG, Alperovitch A, Poser S, Pocchiari M, Hofman A, Mitrova E, et al. Descriptive epidemiology of Creutzfeldt-Jakob disease in six European countries. Ann Neurol 1998;43:763–7.
[4] Duffy P, Wolf J, Collins G, DeVoe AG, Streeten B, Cowen D. Letter: possible person-to-person transmission of Creutzfeldt-Jakob disease. N Engl J Med 1974;290:692–3.
[5] Bernoulli C, Siegfried J, Baumgartner G, Regli F, Rabinowicz T, Gajdusek DC, et al. Danger of accidental person-to-person transmission of Creutzfeldt-Jakob disease by surgery. Lancet 1977;1:478–9.
[6] Koch TK, Berg BO, De Armond SJ, Gravina RF. Creutzfeldt-Jakob disease in a young adult with idiopathic hypopituitarism. Possible relation to the administration of cadaveric human growth hormone. N Engl J Med 1985;313:731–3.
[7] Thadani V, Penar PL, Partington J, Kalb R, Janssen R, Schonberger LB, et al. Creutzfeldt-Jakob disease probably acquired from a cadaveric dura mater graft. Case report. J Neurosurg 1988;69:766–9.
[8] Bruce ME, Will RG, Ironside JW, McConnell I, Drummond D, Suttie A, et al. Transmissions to mice indicate that 'new variant' CJD is caused by the BSE agent. Nature 1997;389:498–501.
[9] Hill AF, Desbruslais M, Joiner S, Sidle KC, Gowland I, Collinge J, et al. The same prion strain causes vCJD and BSE. Nature 1997;389:448–50. 526.
[10] Prusiner SB. Molecular biology of prion diseases. Science 1991;252:1515–22.
[11] Gabizon R, McKinley MP, Groth D, Prusiner SB. Immunoaffinity purification and neutralization of scrapie prion infectivity. Proc Natl Acad Sci USA 1988;85:6617–21.
[12] Heppner FL, Musahl C, Arrighi I, Klein MA, Rulicke T, Oesch B, et al. Prevention of scrapie pathogenesis by transgenic expression of anti-prion protein antibodies. Science 2001;294:178–82.
[13] White AR, Enever P, Tayebi M, Mushens R, Linehan J, Brandner S, et al. Monoclonal antibodies inhibit prion replication and delay the development of prion disease. Nature 2003;422:80–3.
[14] Nashar TO, Amin T, Marcello A, Hirst TR. Current progress in the development of the B subunits of cholera toxin and *Escherichia coli* heat-labile enterotoxin as carriers for the oral delivery of heterologous antigens and epitopes. Vaccine 1993;11:235–40.
[15] Holmgren J, Czerkinsky C, Eriksson K, Mharandi A. Mucosal immunisation and adjuvants: a brief overview of recent advances and challenges. Vaccine 2003;21(Suppl. 2):S89–95.
[16] Tsuji T, Yokochi T, Kamiya H, Kawamoto Y, Miyama A, Asano Y. Relationship between a low toxicity of the mutant A subunit of enterotoxigenic *Escherichia coli* enterotoxin and its strong adjuvant action. Immunology 1997;90:176–82.
[17] Hornemann S, Glockshuber R. Autonomous and reversible folding of a soluble amino-terminally truncated segment of the mouse prion protein. J Mol Biol 1996;261:614–9.
[18] Peretz D, Williamson RA, Kaneko K, Vergara J, Leclerc E, Schmitt-Ulms G, et al. Antibodies inhibit prion propagation and clear cell cultures of prion infectivity. Nature 2001;412:739–43.
[19] Nicotera P. A route for prion neuroinvasion. Neuron 2001;31:345–8.
[20] Ghosh S. Intestinal entry of prions. Z Gastroenterol 2002;40:37–9.
[21] Wilesmith JW, Wells GA, Cranwell MP, Ryan JB. Bovine spongiform encephalopathy: epidemiological studies. Vet Rec 1988;123:638–44.
[22] Llewelyn CA, Hewitt PE, Knight RSG, Amar K, Cousens S, Mackenzie J, et al. Possible transmission of variant Creutzfeldt-Jakob disease by blood transfusion. Lancet 2004;363:417–21.
[23] Peden AH, Head MW, Ritchie DL, Bell JE, Ironside JW. Preclinical vCJD after blood transfusion in a PRNP codon 129 heterozygous patient. Lancet 2004;364:527–9.
[24] Goni F, Knudsen E, Schreiber F, Scholtzova H, Pankiewicz J, Carp R, et al. Mucosal vaccination delays or prevents prion infection via an oral route. Neuroscience 2005;133:413–21.
[25] Behar SM, Porcelli SA. Mechanisms of autoimmune disease induction. The role of the immune response to microbial pathogens. Arthritis Rheum 1995;38:458–76.
[26] Ang CW, Jacobs BC, Laman JD. The Guillain-Barre syndrome: a true case of molecular mimicry. Trends Immunol 2004;25:61–6.
[27] Koller MF, Grau T, Christen P. Induction of antibodies against murine full-length prion protein in wild-type mice. J Neuroimmunol 2002;132:113–6.
[28] Rosset MB, Ballerini C, Gregoire S, Metharom P, Carnaud C, Aucouturier P. Breaking immune tolerance to the prion protein using prion

protein peptides plus oligodeoxynucleotide-CpG in mice. J Immunol 2004;172:5168–74.

[29] Gilch S, Wopfner F, Renner-Muller I, Kremmer E, Bauer C, Wolf E, et al. Polyclonal anti-PrP auto-antibodies induced with dimeric PrP interfere efficiently with PrPSc propagation in prion-infected cells. J Biol Chem 2003;278:18524–31.

[30] Nikles D, Bach P, Boller K, Merten CA, Montrasio F, Heppner FL, et al. Circumventing tolerance to the prion protein (PrP): vaccination with PrP-displaying retrovirus particles induces humoral immune responses against the native form of cellular PrP. J Virol 2005;79:4033–42.

JOURNAL OF VIROLOGY, Aug. 2006, p. 7854–7862
0022-538X/06/$08.00+0 doi:10.1128/JVI.00424-06

Vol. 80, No. 16

Prion Strain-Dependent Differences in Conversion of Mutant Prion Proteins in Cell Culture

Ryuichiro Atarashi,[1,2]* Valerie L. Sim,[2] Noriyuki Nishida,[1] Byron Caughey,[2] and Shigeru Katamine[1]

Department of Molecular Microbiology and Immunology, Nagasaki University Graduate School of Biomedical Sciences, 1-12-4 Sakamoto, Nagasaki 853-8523, Japan,[1] and Laboratory of Persistent Viral Diseases, Rocky Mountain Laboratories, National Institute of Allergy and Infectious Diseases, National Institutes of Health, Hamilton, Montana 59840[2]

Received 28 February 2006/Accepted 19 May 2006

Although the protein-only hypothesis proposes that it is the conformation of abnormal prion protein (PrP^{Sc}) that determines strain diversity, the molecular basis of strains remains to be elucidated. In the present study, we generated a series of mutations in the normal prion protein (PrP^{C}) in which a single glutamine residue was replaced with a basic amino acid and compared their abilities to convert to PrP^{Sc} in cultured neuronal N2a58 cells infected with either the Chandler or 22L mouse-adapted scrapie strain. In mice, these strains generate PrP^{Sc} of the same sequence but different conformations, as judged by infrared spectroscopy. Substitutions at codons 97, 167, 171, and 216 generated PrP^{C} that resisted conversion and inhibited the conversion of coexpressed wild-type PrP in both Chandler-infected and 22L-infected cells. Interestingly, substitutions at codons 185 and 218 gave strain-dependent effects. The Q185R and Q185K PrP were efficiently converted to PrP^{Sc} in Chandler-infected but not 22L-infected cells. Conversely, Q218R and Q218H PrP were converted only in 22L-infected cells. Moreover, the Q218K PrP exerted a potent inhibitory effect on the conversion of coexpressed wild-type PrP in Chandler-infected cells but had little effect on 22L-infected cells. These results show that two strains with the same PrP sequence but different conformations have differing abilities to convert the same mutated PrP^{C}.

Transmissible spongiform encephalopathies (TSE), or prion diseases, are lethal neurodegenerative diseases that include Creutzfeldt-Jakob disease in humans, scrapie in sheep, and bovine spongiform encephalopathy in cattle. The infectious agent, termed prion, is unique in that no agent-specific nucleic acid is detectable. The protein-only hypothesis proposes that this agent consists solely of an abnormal form of prion protein (PrP^{Sc}), which is produced by the conversion of the normal cellular prion protein (PrP^{C}) and accumulates primarily in the lymphoreticular and central nervous system during the course of prion disease (41, 56). PrP^{C}, a host-encoded glycoprotein anchored to the cell membrane by a glycosyl-phosphatidylinositol moiety, is expressed mainly in the central nervous system. PrP^{C} is detergent soluble and proteinase K (PK) sensitive, whereas PrP^{Sc} is detergent insoluble and partially PK resistant (35). These different biophysical properties are thought to be due to different conformations of the two isoforms. PrP^{C} is highly α-helical, but PrP^{Sc} has a large proportion of β-sheet structure (14, 38).

Various TSE strains with distinct biological characteristics have been identified in several mammalian species. These strains are characterized by different incubation periods and histopathological changes (9, 10). Generally, the phenotypic characteristics are maintained upon repeated passages in the same species with the same PrP amino acid sequence. In addition, previous reports showed that strain-specific biological characteristics remain unchanged after passages in cell cultures (2, 8). In contrast, changing to a species with a different PrP sequence often results in the emergence of a new strain (28, 29). The existence of multiple strains signifies that the infectious agent carries some form of strain-specific information that determines each strain's characteristics. One possibility is that this information stems from the distinct PrP^{Sc} conformation of each strain. Differences in the electrophoretic mobilities of PK-resistant PrP^{Sc} core fragments among strains are well documented (7, 16, 50). These different-sized PrP^{Sc} fragments are likely a consequence of differing conformations and thus different PK cleavage points. Conformational differences in β-sheet structures between strains have also been demonstrated by infrared (IR) spectroscopy (13, 52). Furthermore, Syrian hamster (SHa) PrP^{Sc}, when denatured, binds more anti-PrP antibody than when it is in its native form, and each strain can have distinct denatured versus nondenatured binding ratios (44). In addition, some Syrian hamster TSE strains are reported to differ in the extent of their PK resistance after partial denaturation with guanidine hydrochloride (39). These findings support the hypothesis that TSE strains have distinct PrP^{Sc} conformations. Moreover, cell-free conversion experiments have shown that different forms of PrP^{Sc} can induce strain-specific conformational changes in PrP^{C} (6), and Jones and Surewicz recently reported that artificial amyloid fibrils of PrP23-144 from different species revealed strain-like behavior in vitro (25). Nevertheless, much remains to be learned about the mechanistic relationship between PrP^{Sc} conformational differences and the molecular basis of TSE strains.

Studies using transgenic mice and congenic mice have shown that several TSE strains differ in incubation periods in the same host (11, 23, 32). The molecular basis of this remains unresolved, but the conformation of PrP^{Sc} could influence incubation periods by affecting the efficiency and location of

* Corresponding author. Mailing address: Laboratory of Persistent Viral Diseases, Rocky Mountain Laboratories, NIAID, NIH, 903 South 4th Street, Hamilton, MT 59840. Phone: (406) 363-9341. Fax: (406) 363-9286. E-mail: atarashir@niaid.nih.gov.

PrP^{Sc} formation. However, to date, there are little data on the influence of PrP mutations on PrP^{Sc} formation in vitro.

Because N2a58 cells overexpressing mouse PrP can be persistently infected with the Chandler or 22L prion strain (37), we chose to examine the strain-specific effect of PrP mutations on PrP^{Sc} formation in N2a58 cell cultures infected with the Chandler or 22L strain, designated Ch-N2a58 and 22L-N2a58, respectively. Although little is known about which amino acid residues of the PrP sequence correlate with the strain-specific formation of PrP^{Sc}, we noticed that mutations from glutamine to arginine or lysine in the C terminus of the PrP were related to the resistance of prion diseases (4, 47, 57) and inhibited the conversion of coexpressed wild-type PrP in Chandler-infected N2a cell cultures (26). In this study, we created a series of PrP mutations in which a single glutamine residue was replaced with an arginine residue and compared the effects of these mutations on PrP^{Sc} formation in Ch- and 22L-N2a58 cells. We demonstrated that specific amino acids residues in PrP^{C} can allow or inhibit PrP^{Sc} formation in vitro for one strain but not another even though the amino acid sequence of PrP^{Sc} is the same in each strain. Our results suggest that each prion strain can interact with PrP^{C} in a strain-specific manner, producing PrP^{Sc} with a strain-specific conformation and unique biological characteristics.

MATERIALS AND METHODS

Cell culture. N2a58 cells overexpressing mouse PrP (PrP-a genotype, codons 108L and 189T) were prepared as described previously (37). To create N2a58 cells infected with either the Chandler/RML or 22L strain (Ch-N2a58 and 22L-N2a58), the cells were incubated with brain homogenates from ddY mice infected with each strain. After subcloning by limiting dilution, several PrP^{Sc}-positive clones were isolated. The cell clones producing the highest level of PrP^{Sc} were used for subsequent study. Both Ch-N2a58 and 22L-N2a58 cells stably expressed PrP^{Sc} for over 50 passages. Morphological appearances and growth characteristics of these prion-infected cells were indistinguishable from those of N2a58 cells (data not shown). All cells were cultured in Opti-MEM (Invitrogen) containing 10% fetal bovine serum and penicillin-streptomycin at 37°C in 5% CO_2 and were split every 3 to 4 days at an 8- to 10-fold dilution.

Plasmid constructions. The open reading frames of Syrian hamster PrP (SHa), human PrP (Hu), and mouse PrP containing the epitope for the 3F4 antibody (Mo3F4) were amplified by PCR with mouse DNA, MHM2/Mo3F4 PrP transgenic mouse DNA, SHa PrP transgenic mouse (3) DNA, and human DNA, respectively. Amplified fragments were inserted into the pcDNA3.1(+) vector (Invitrogen) between the BamHI and XbaI sites. Mouse PrP (PrP-a genotype) containing the epitope for the L42 antibody (MoL42) was introduced into mouse PrP by PCR-direct mutagenesis.

Mo3F4 PrP differs from the mouse PrP-a genotype by two amino acids, L108M and V111M, which are included in the epitope recognized by the 3F4 anti-PrP monoclonal antibody (Dako). MoL42 PrP has one amino acid substitution, W144Y, which is recognized by the L42 anti-PrP antibody (R-biopharm) (54). Since neither antibody reacts with mouse PrP, transfected recombinant PrP is distinguishable from endogenous mouse PrP.

Mo3F4 sequences with specific amino acid changes (Q90R, Q97R, Q159R, Q167R, Q171R, Q185R, Q185K, Q185H, Q185E, Q185L, Q211R, Q216R, Q218R, Q218K, Q218H, Q218E, Q218L, and Q222R) were generated by PCR mutagenesis. The resulting PCR fragments were subcloned into the pcDNA3.1(+) vector. To create MoL42 mutations with specific amino acid changes (Q185R, Q218R, Q218K, and Q218H), BamHI-BstPI fragments of the corresponding Mo3F4 mutants in the pcDNA3.1(+) vector were replaced by those of MoL42 PrP. The PrP sequences of all plasmids used in this study were confirmed by using the ABI PRISM 3100 genetic analyzer (Applied Biosystems), and no unexpected mutations were found.

Transfection and Western blotting. N2a58, Ch-N2a58, and 22L-N2a58 cells were transiently transfected with various plasmid constructs (1 or 2 μg DNA per 6-cm dish) using the Effectene transfection reagent (QIAGEN) according to the manufacturer's instructions. To evaluate dominant-negative inhibition of PrP^{Sc} formation, cotransfections of two different PrP constructs were performed with a DNA ratio of 1:1 or 1:2. Indirect immunofluorescence of PrP and fluorescence imaging of pEGFP-C1 (Clontech) revealed that transfection efficiencies were around 40 to 60% and that the rate of the overlapping expression of two plasmids cotransfected was more than 90%.

After 72 h of transfection, cells from a 6-cm dish were lysed in 0.5 ml of lysis buffer (150 mM NaCl, 50 mM Tris-HCl [pH 7.5], 0.5% Triton X-100, 0.5% sodium deoxycholate, and 1 mM EDTA). After cell debris and nuclei were removed by low-speed centrifugation, the protein concentration of the supernatant was measured by the BCA protein assay (Pierce). To detect PrP^{Sc}, the protein concentration of the supernatant was adjusted with lysis buffer to 1 mg/ml. Samples of equal protein concentrations and volumes were digested with 20 μg/ml of proteinase K at 37°C for 45 min, and the digestion was stopped by adding phenylmethylsulfonyl fluoride (2 mM). After 60 min of centrifugation at 20,400 × *g*, the pellet was dissolved with sample buffer (4 M urea, 4% sodium dodecyl sulfate, 100 mM dithiothreitol, 10% glycerol, 0.02% bromophenol blue, and 50 mM Tris-HCl [pH 6.8]), boiled, and then loaded onto a 15% polyacrylamide gel. Proteins were transferred onto a membrane (Immobilon P; Millipore). 3F4-positive PrPs were detected with 3F4 antibody, L42-positive PrPs were detected with L42 antibody, and total PrP was detected with mouse polyclonal anti-PrP antibody (designated SS). Immunoreactive bands were visualized using the ECL detection system (Amersham Biosciences). The expression level of transfected PrP in cell lysates (30 μg of total protein per lane) was also estimated by immunoblotting. Densitometric analysis of the film was performed using NIH Image software. The conversion efficiency of Mo3F4 was assigned as 100%, and the level of PrP^{Sc} formation in each 3F4-positive mutant was calculated relative to this value. In some experiments, the cell lysates with proteinase K treatment were digested with PNGase F (New England Biolabs).

IR spectroscopy of PrP^{Sc}. PrP^{Sc} was isolated from the brains of mice affected by either 22L, Chandler, or 87V scrapie and treated with PK as described previously (13). For IR analysis, ~3 μl of pelleted slurries containing at least 10 mg/ml PrP^{Sc} in a solution containing 20 mM sodium phosphate, 130 mM NaCl (pH 7.5), and 0.5% sulfobetaine was applied to a Golden Gate Single Reflection Diamond Attenuated Total Reflectance unit purged with dry air and covered to prevent sample evaporation. Data collection was performed using a System 2000 IR instrument (Perkin-Elmer). Test conditions were as follows: 20°C, 4.00-cm^{-1} resolution, 2-cm/s optical path difference velocity, 1,000 scans, and 0.5-cm^{-1} data interval. The detector was an nb1 MCT detector cooled by liquid nitrogen. Primary spectra were obtained by subtracting the spectra of the corresponding buffer or buffer with additives and water vapor and by adjusting the baseline and normalizing for comparable absorbance of different concentrations of PrP. Second-derivative spectra were calculated from the primary spectra using 13 data points. The software used for spectral analyses was Spectrum v2.00 (Perkin-Elmer).

RESULTS

Mo3F4 PrP converts to PrP^{Sc} with similar efficiency in Ch-N2a58 and 22L-N2a58 cells. Prior to creating PrP mutants, we first confirmed that our starting Mo3F4 vector could convert to PrP^{Sc} in cells persistently infected with the Chandler or 22L mouse-adapted scrapie strain (Ch-N2a58 and 22L-N2a58 cells, respectively). The presence of endogenous mouse PrP^{Sc} in the Ch-N2a58 and 22L-N2a58 cells was confirmed by immunoblotting with the mouse polyclonal anti-PrP SS antibody. Similar amounts of endogenous mouse PrP^{Sc} accumulated in Ch-N2a58 and 22L-N2a58 cells, while none was detected in uninfected N2a58 cells (Fig. 1A). In the transfected cells, PK-resistant PrP^{Sc} derived from Mo3F4 PrP was distinguished from endogenous mouse PrP^{Sc} by immunoblotting with the monoclonal anti-PrP 3F4 antibody (Fig. 1B). PK-resistant PrP^{Sc} core fragments from Ch-N2a58 and 22L-N2a58 cells were treated with PNGase F to remove asparagine-linked glycosylation and immunoblotted with either SS or 3F4 antibody. No differences in gel migration patterns were seen (Fig. 1C).

Q218K PrP does not convert and inhibits PrP^{Sc} formation from coexpressed Mo3F4 PrP in Ch-N2a58 but not in 22L-N2a58 cells. In order to compare the consequences of changes in the PrP primary structure between Ch-N2a58 and 22L-

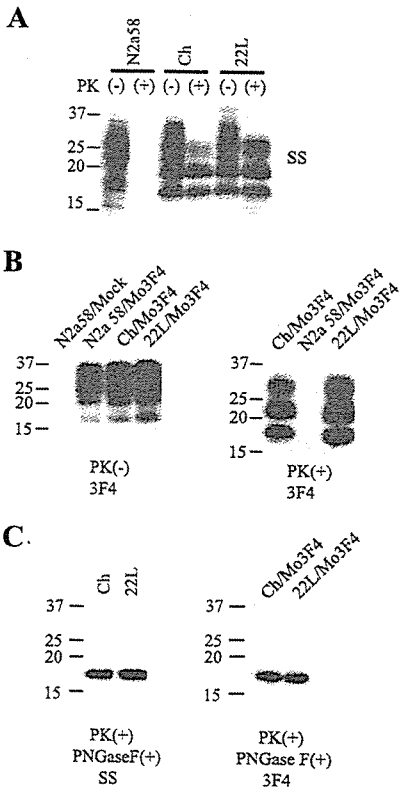

FIG. 1. Formation of Mo3F4-derived PrP^{Sc} in Ch-N2a58 and 22L-N2a58 cells. (A) Western blot using polyclonal anti-PrP antibody SS in N2a58, Ch-N2a58 (Ch), and 22L-N2a58 (22L) cells without (−) or with (+) PK treatment. (B) Expression levels of Mo3F4 PrP (left panel) and detection of Mo3F4-derived PrP^{Sc} (right panel) were measured by Western blot using monoclonal antibody 3F4. Mock, untransfected cells. (C) After consecutive treatments of PK and PNGase F, untransfected (left panel) and Mo3F4 PrP-transfected cells (right panel) were analyzed by Western blotting using SS and 3F4 antibodies, respectively. Molecular mass markers are indicated in kilodaltons on the left side of each panel.

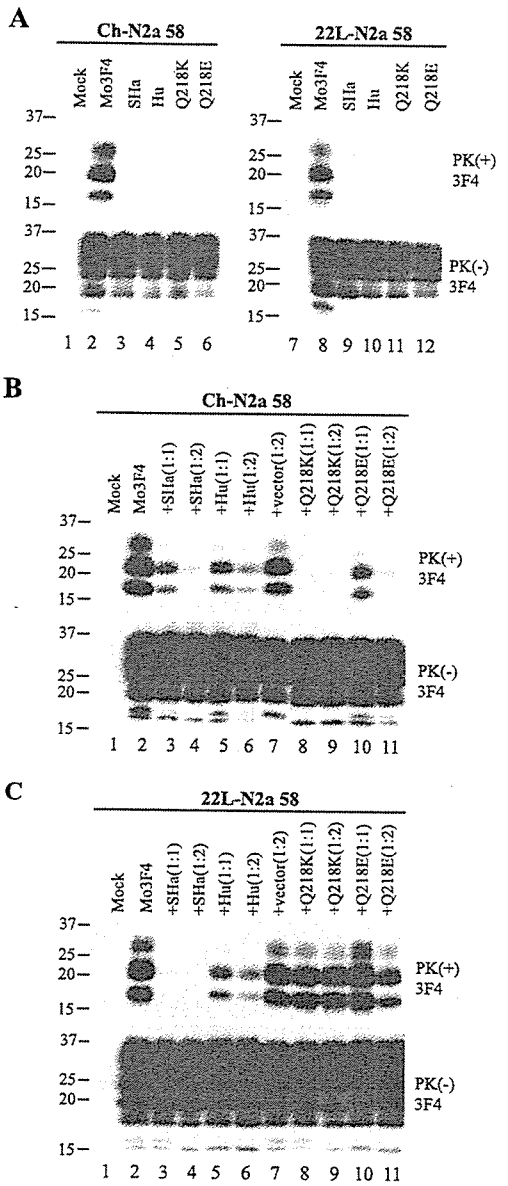

FIG. 2. Strain-dependent inhibitory effect of Q218K mutation on PrP^{Sc} formation of wild-type Mo3F4. (A) Conversion to 3F4-positive PrP^{Sc} (upper panels) and expression of Mo3F4, SHa, Hu, Q218K, and Q218E (lower panels) were measured by Western blot using 3F4 antibody. The 3F4 epitope was present in all these constructs. (B and C) The inhibitory effect of the constructs was determined by cotransfection with Mo3F4 in the DNA ratio of 1:1 or 1:2. The blots were probed with 3F4 antibody. Mock, untransfected cells; +vector(1:2), cotransfection of Mo3F4 and pcDNA3.1(+) at a 1:2 ratio.

N2a58 cells, we first examined the PrP^{Sc} formation of two heterologous PrPs, Syrian hamster (SHa) and human (Hu) PrPs, and two Mo3F4 mutated PrPs with a single amino acid substitution at codon 218, Q218K and Q218E, in the infected cells transfected with the corresponding expression vectors. The 3F4 antibody detected SHa, Hu, and Mo3F4 mutated PrPs expressed in Ch-N2a58 and 22L-N2a58 cells at a level similar to that of wild-type Mo3F4 PrP (Fig. 2A, lower panels). SHa, Hu, Q218K, and Q218E PrP did not convert to PrP^{Sc} in Ch-N2a58 (Fig. 2A, upper panel, lanes 3 to 6) and 22L-N2a58 (Fig. 2A, upper panel, lanes 9 to 12) cells.

To evaluate the inhibitory effect of these heterologous and mutated PrPs, each expression vector was cotransfected with that of Mo3F4 PrP at a DNA ratio of 1:1 or 1:2. As seen previously (26), in Ch-N2a58 cells, Q218K PrP completely inhibited the accumulation of PrP^{Sc} derived from Mo3F4 PrP even at a DNA ratio of 1:1 (Fig. 2B, upper panel, lanes 8 and 9). SHa, Hu, and Q218E PrP also revealed a dose-dependent inhibitory effect but to a lesser extent (Fig. 2B, upper panel, lanes 3 to 6, 10, and 11). In remarkable contrast, in 22L-N2a58 cells, Q218K PrP had little effect on Mo3F4 PrP^{Sc} accumulation (Fig. 2C, upper panel, lanes 8 and 9). The inhibitory effect of Q218E PrP in 22L-N2a58 cells was also very weak (Fig. 2C, upper panel, lanes 10 and 11). Conversely, SHa PrP inhibited Mo3F4-derived PrP^{Sc} formation to a greater extent in 22L-N2a58 cells than in Ch-N2a58 cells (Fig. 2C, upper panel, lanes 3 and 4). These results were reproduced in three independent experiments (Table 1). These data suggest that the inhibition